Proc. Natl. Acad. Sci. USA
Vol. 93, pp. 799–803, January 1996
Biochemistry

Toward antibody-directed "abzyme" prodrug therapy, ADAPT: Carbamate prodrug activation by a catalytic antibody and its *in vitro* application to human tumor cell killing

PAUL WENTWORTH*†, ANITA DATTA*, DAVID BLAKEY‡, TOM BOYLE‡, LYNDA J. PARTRIDGE*, AND G. MICHAEL BLACKBURN*§

*Departments of Chemistry and Molecular Biology, Krebs Institute for Biomolecular Research, University of Sheffield, Sheffield, S3 7HF, United Kingdom; and ‡Cancer Research Department, Zeneca Ltd., Alderley Park, Macclesfield, Cheshire, SK10 4TG, United Kingdom

Communicated by Richard A. Lerner, Scripps Research Institute, La Jolla, CA, October 10, 1995

ABSTRACT **Antibody-directed enzyme prodrug therapy, ADEPT, is a recent approach to targeted cancer chemotherapy intended to diminish the nonspecific toxicity associated with many commonly used chemotherapeutic agents. Most ADEPT systems incorporate a bacterial enzyme, and thus their potential is reduced because of the immunogenicity of that component of the conjugate. This limitation can be circumvented by the use of a catalytic antibody, which can be "humanized," in place of the bacterial enzyme catalyst. We have explored the scope of such antibody-directed "abzyme" prodrug therapy, ADAPT, to evaluate the potential for a repeatable targeted cancer chemotherapy. We report the production of a catalytic antibody that can hydrolyze the carbamate prodrug 4-[*N,N*-bis(2-chloroethyl)]aminophenyl-*N*-[(1*S*)-(1,3-dicarboxy)propyl]carbamate (1) to generate the corresponding cytotoxic nitrogen mustard (K_m = 201 μM, k_{cat} = 1.88 min^{-1}). *In vitro* studies with this abzyme, EA11-D7, and prodrug 1 lead to a marked reduction in viability of cultured human colonic carcinoma (LoVo) cells relative to appropriate controls. In addition, we have found a good correlation between antibody catalysis as determined by this cytotoxicity assay *in vitro* and competitive binding studies of candidate abzymes to the truncated transition-state analogue ethyl 4-nitrophenylmethylphosphonate. This cell-kill assay heralds a general approach to direct and rapid screening of antibody libraries for catalysts.**

Antibody-directed enzyme prodrug therapy, ADEPT, has been developed to overcome the unwanted nonspecific toxicity associated with anticancer agents (1–5). There are two components to such therapy: an antibody-enzyme conjugate and an anticancer prodrug of low toxicity. The conjugate is administered first and accumulates predominantly at the tumor site through antibody binding to tumor-associated antigenic determinants. Once the conjugate has been cleared from the plasma, the prodrug is administered to the patient. Cleavage of the prodrug to generate the active cytotoxic agent by the enzyme component of the conjugate occurs *selectively* at the tumor site and so leads both to enhanced efficacy of the anticancer agent and to reduced peripheral cytotoxicity (Fig. 1).

To diminish the extent of peripheral hydrolysis of the prodrug, the enzyme component selected has commonly been of bacterial origin in order to achieve the necessary degree of specificity of activation (3): a human enzyme would be less specific. Unfortunately, such a choice imposes a dose-limiting immunogenicity on the ADEPT conjugate which could reduce the clinical potential of this therapy (6).

Antibodies generated against appropriate transition-state analogues (TSAs) can catalyze a variety of chemical transformations (7, 8). Furthermore, murine antibodies can be "humanized" by existing technologies to reduce their inherent *in vivo* mammalian immunogenicity (9). These concepts have been juxtaposed by Bagshawe (6), who has proposed that humanized catalytic antibodies ("abzymes") could replace the enzyme component of ADEPT in an improved targeted therapy. We here demonstrate the feasibility of that proposition, which we have named antibody-directed abzyme prodrug therapy, ADAPT. We have identified an antibody that can efficiently hydrolyze a carbamate prodrug and so effect cytotoxicity *in vitro*. This provides a major extension to the potential for application of catalytic antibodies to clinical therapy.

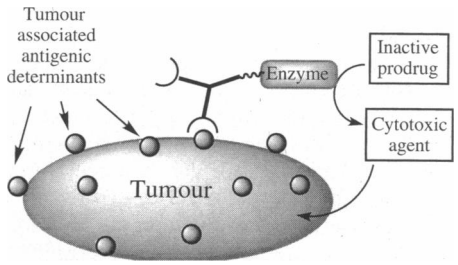

FIG. 1. Schematic representation of ADEPT.

Our TSA design takes account of three requirements. First, we needed antibodies that could operate on carbamates derived from L-glutamic acid (Fig. 2) to permit direct comparisons of antibody performance with those of the bacterial CPG2 exopeptidase enzyme previously reported to convert this prodrug and give antitumor activity (10). Second, the locus of the nitrogen mustard in prodrug **1** was selected to define the position of the linker arm in order to minimize prodrug alkylation of the abzymes. Third, we chose to promote the disfavored $B_{AC}2$ mechanism¶ of carbamate hydrolysis rather than the spontaneous E1cB process to obtain the maximum catalytic rate enhancement for a weakly acidic phenol leaving group (11). Accordingly, a phosphonamidate tetrahedral center (12) was chosen to mimic the high-energy intermediate for

The publication costs of this article were defrayed in part by page charge payment. This article must therefore be hereby marked "*advertisement*" in accordance with 18 U.S.C. §1734 solely to indicate this fact.

Abbreviations: ADEPT, antibody-directed enzyme prodrug therapy; ADAPT, antibody-directed abzyme prodrug therapy; BSA, bovine serum albumin; KLH, keyhole limpet hemocyanin; LDMS, laser desorption mass spectrometry; mAb, monoclonal antibody; SPR, surface plasmon resonance; SRB, sulforhodamine B; TNBS, 2,4,6-trinitrobenzenesulfonic acid; TSA, transition-state analogue.

†Present address: Department of Molecular Biology, The Scripps Research Institute, 10666 North Torrey Pines Road, La Jolla, CA 92037.
§To whom reprint requests should be addressed.

¶In-depth kinetic evaluation of one antibody raised against phosphonamidate **3**, including Hammett σ–ρ correlations for a series of aryl carbamate ester substrates, has been used to show that the abzyme catalyzes cleavage of carbamates by the normally disfavored $B_{AC}2$ mechanism of hydrolysis. These results will be reported elsewhere.

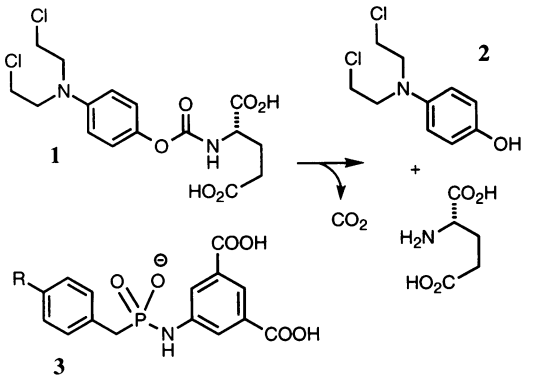

FIG. 2. Prodrug **1** is cleaved to release the cytotoxic agent **2**. Phosphonamidate **3** is the designed TSA.

the $B_{AC}2$ cleavage process in anticipation that its N—H group might also promote selection in favor of a hydrogen bond donor–acceptor system in the abzyme for enhanced transition-state stabilization. According to recent reports the hydrolysis of an activated carbamate ester can be accelerated by antibodies elicited to a phosphonate TSA (13).

Finally, we designed a phosphonamidate **3** based on 5-aminoisophthalic acid to create a stable, entropically limited mimic of one rotamer of the glutamic acid prodrug **1**.

Immunizations were performed with the conjugate of the anionic phosphonamidate **5** (see Fig. 3) and independently with that of the neutral ester **4** to establish the charge requirements of TSAs for carbamate ester hydrolysis, since other reports have shown that antibodies elicited to neutral tetrahedral phosphonates (14) or secondary alcohols (15) can catalyze acyl transfer reactions.

MATERIALS AND METHODS

Materials. The parent drug, 4-[*N,N*-bis(2-chloroethyl)]-aminophenol (**2**), and carbamate prodrug, 4-[*N,N*-bis(2-chloroethyl)]aminophenyl-*N*-[(1*S*)-(1,3-dicarboxy)propyl]carbamate (**1**), were gifts from Zeneca (Macclesfield, U.K.).

Instrumentation. The technique of surface plasmon resonance (SPR) was implemented on a Pharmacia BIAcore instrument to make real-time kinetic measurements of antibody binding to transition state analogues immobilized on a carboxymethylated dextran-coated surface of a CM5 sensor chip (Pharmacia Biosensor) (16).

Hapten Synthesis. Ethyl *N*-(3,5-dicarboxyphenyl)-*P*-{*N*-[5′-(2″,5″-dioxo-1″-pyrrolidinyl)oxy-1′,5′-dioxopentyl]-4-aminophenylmethyl}phosphonamidate (**4**) was synthesized in six steps from commercially available diethyl phosphite and 4-nitrophenylmethyl bromide. The phosphonamidic acid **5** was prepared by phosphorus deesterification of **4**, using bromotrimethylsilane. Full experimental details of the reaction scheme outlined in Fig. 3 will be reported elsewhere. The *N*-hydroxysuccinimide esters were used to link the haptens to keyhole limpet hemocyanin (KLH) and bovine serum albumin (BSA) carrier proteins (Imject grade, Pierce).

Hapten Density Determination. In addition to a standard SDS/PAGE method (17), the KLH and BSA conjugates of haptens **4** and **5** were analyzed by Habeeb's 2,4,6-trinitrobenzenesulfonic acid (TNBS) assay (18), used with a reaction time shortened to minimize photolytic side reactions. The BSA conjugates were more accurately analyzed by matrix-assisted laser desorption mass spectrometry (LDMS) (19) using a Finnigan MAT LDMS machine with an IBM 486 workstation and a cinnamic acid matrix; samples were rigorously desalted to minimize signal suppression.

Antibody Generation. Female BALB/c mice were hyperimmunized with the KLH immunoconjugates of **4** and **5** by standard procedures (20) until the serum titers were greater than 20,000. Hybridoma cell lines were then generated (21–23), and selection was made on the basis of recognition of the appropriate TSA. Hybridoma cell lines secreting antibodies specific for the TSA were expanded in culture flasks and purified in a two-step procedure involving ammonium sulfate precipitation and protein-G column chromatography. All antibody preparations were assessed for purity by SDS/PAGE chromatography under reducing conditions (17).

Hybridoma Characterization. Apparent affinity constants (a*K*) were measured with an inhibition displacement ELISA based on the method of Nieto *et al.* (24), using the BSA

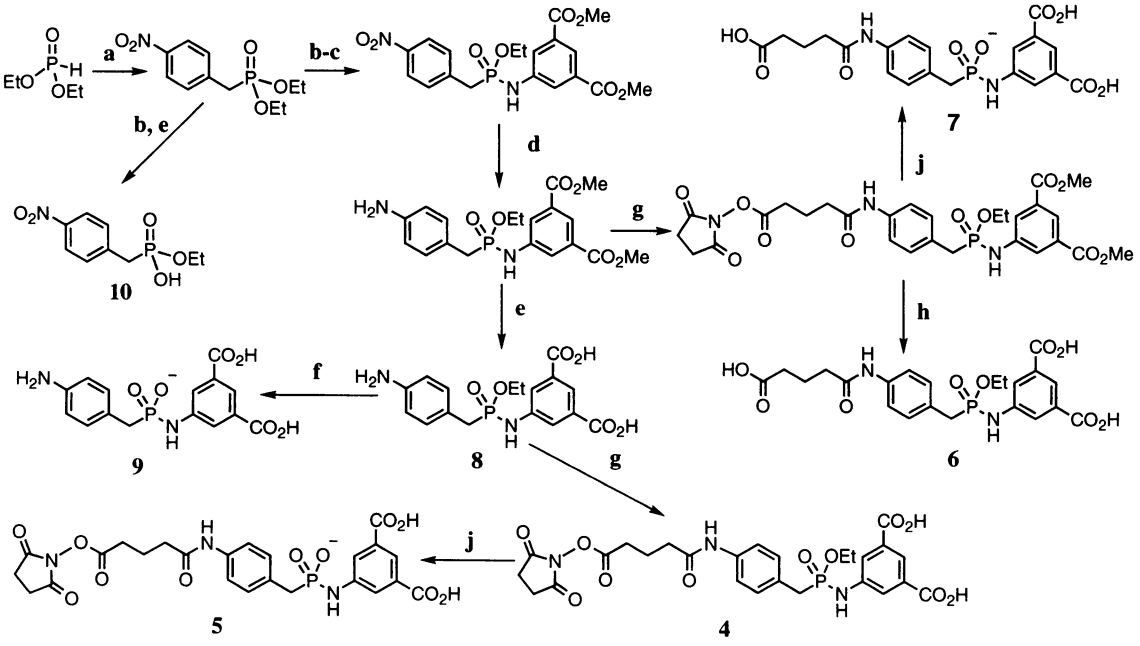

FIG. 3. Hapten synthesis. Step a, Na/4-nitrobenzyl bromide; step b, PCl_5; step c, dimethyl 5-aminoisophthalate/Et_3N, 4-dimethylaminopyridine (DMAP); step d, H_2/Adams catalyst; step e, NaOH (aq); step f, bromotrimethylsilane (TMSBr)/$NaHCO_3$ solvolysis; step g, 5-(2′,5′-dioxo-1′-pyrrolidinyl)oxy-5-oxopentanoyl chloride/Et_3N; step h, LiOH (aq); and step j, TMSBr (8 eq), 35–40°C.

immunoconjugates of **4** and **5** in conjunction with their parent acids **6** and **7**, respectively. The free aminophenyl TSAs, **8** and **9**, were immobilized on a CM5 sensor chip for determination of affinity constants (K_a) by using a BIAcore system (16). Solutions were injected onto the chip at a constant flow rate (5 $\mu l \cdot min^{-1}$). The hydrogel was activated by an *N*-hydroxysuccinimide (0.05 M)/1-(3-dimethylaminopropyl)-3-ethylcarbodiimide (0.2 M) aqueous solution (35 μl). Injection of the ligand (**8** or **9**), diluted in sodium acetate buffer (pH 4, 100 $\mu g \cdot ml^{-1}$, 35 μl), was followed by ethanolamine hydrochloride (pH 8.5, 1 M, 25 μl) to deactivate any remaining sites, thus allowing calculation of the immobilization yield in resonance units (RU). The amount of TSA immobilized was adjusted such that the antibody response at surface saturation was between 500 and 1700 RU. The test antibody solutions, prepared at a range of dilutions (50–1000 $ng \cdot ml^{-1}$) in Hepes-buffered saline (HBS; 50 mM Hepes, pH 8.0/0.9% NaCl), were assessed in turn by injection into the BIAcore system (25 μl), allowing measurement of the association phase kinetics. Pure HBS (25 μl) was injected to enable measurement of the kinetics of the dissociation phase. In the case of displacement studies, various concentrations of competing ligand—e.g., **10**—were injected during the association phase to produce an accelerated dissociation phase during HBS elution. Finally, injection of HCl (50 mM, 6 μl) served to remove all noncovalently linked material from the surface, thus regenerating the sensor chip for the next run.

Antibody Isotyping. Isotyping was performed early in the lifetime of the cell lines by using both ELISA and SPR methods. Of 55 cell lines elicited to haptens **4** and **5**, the majority are IgG1, with 12% IgG2a, and a single IgM (BG11). EA11-D7 is of IgG1 isotype.

EA11-D7 Fab Preparation. A purified EA11-D7 solution was concentrated to 15 $mg \cdot ml^{-1}$ by using a Microcon filter. This solution was then dialyzed into sodium acetate (100 mM, pH 5.5). Cysteine (0.25 ml, 1 M) and ethylenediaminetetraacetic acid (0.25 ml, 25 mM) were added to this solution (5 ml) in an Eppendorf tube. Papain (EC 3.4.22.2) immobilized on agarose beads (Sigma, 140 μg, 0.6 unit) was then added, and the tube was sealed and incubated overnight at 37°C. The EA11-D7 Fab was isolated by centrifugation of the solution to remove the immobilized papain and purification of the supernatant by protein-G column chromatography.

Sulforhodamine B (SRB) Assay. Monoclonal antibodies (mAbs) were screened for their ability to activate the carbamate prodrug **1** in a modification of the SRB assay of Skehan *et al.* (25). On day 1, 100 μl of LoVo cells [in Dulbecco's modified Eagle's medium (DMEM) with 10% fetal calf serum/2% penicillin/streptomycin/1% glutamine] at $\approx 2.5 \times 10^4$ cells per ml was put into each well of 96-well microtiter plates. The cells were incubated overnight at 37°C with a 5% (vol/vol) CO_2 atmosphere. On day 2, 20 μl of antibody solution at ≈ 1 $mg \cdot ml^{-1}$ (in phosphate-buffered saline, PBS; 9.6 mM sodium phosphate, pH 7.0/0.14 M NaCl) stock concentration, followed by 100 μl of the prodrug **1** (22 μM in DMEM), was added to the test wells while control wells were treated with 20 μl of PBS and 100 μl of DMEM. The plates were then incubated for 1 h at 37°C (5% CO_2). The medium was replaced with 200 μl of complete DMEM and the plates were reincubated under the same conditions for a further 4 days. On day 6, 50 μl of cold trichloroacetic acid (50%) was added to each well. The plates were then incubated at 4°C for 1 h. The supernatant was removed by flicking the plates and repeatedly rinsing with water. SRB dye (100 μl, 0.4% in 1% acetic acid) was then added to the plates, which were incubated at 37°C. The SRB was removed by flicking the plates and repeatedly washing with acetic acid. The plates were allowed to dry at room temperature, Tris·HCl buffer (pH 9.7, 100 μl, 10 mM) was added to each well, and the plates were covered and shaken for 30 min. The absorbances were then measured at 540 nm. The mean A_{540} changes of the test samples ($n = 16$) were compared with the controls, and the percentage difference in mean A_{540} changes were plotted versus antibody concentration.

Determination of Antibody Kinetic Parameters. The concentration of stock antibody was determined by measuring A_{280}, where $\varepsilon_{280} = 195{,}000\ M^{-1} \cdot cm^{-1}$ if the molecular weight of IgG is taken as 150,000. For solutions of prodrug **1**, the rate of hydrolysis was determined by the A_{266} changes for loss of the carbamate ($\varepsilon_{266} = 16{,}000\ M^{-1} \cdot cm^{-1}$) and formation of 4-[*N*,*N*-bis(2-chloroethyl)]aminophenol ($\varepsilon_{266} = 4720\ M^{-1} \cdot cm^{-1}$; $\Delta\varepsilon_{266} = -11{,}280\ M^{-1} \cdot cm^{-1}$) in PBS with a thermostatically controlled Philips PU8720 UV/visible spectrophotometer at 37°C ± 0.1°C. The antibody concentration was 0.64 μM and the prodrug **1** concentration varied from 20 to 500 μM. Antibody catalysis of the reaction was characterized by measuring initial rates from the UV absorbance change corresponding to the first ≈4% of the reaction. These data were then corrected for the background reaction and subjected to a nonlinear regression analysis using the EnzFit computer program (34) to determine values of K_m and k_{cat}. Products (glutamate and **2**) were analyzed by a combination of UV and HPLC data.

RESULTS AND DISCUSSION

The success of conjugating the TSAs **4** and **5** (Fig. 3) to KLH and BSA was assessed by two quantitative techniques. Habeeb's UV assay (18) determines the number of free lysine residues on the hapten-conjugated protein by reaction of its unsubstituted lysines with TNBS and gives the *average* number of haptens per carrier protein (Table 1). The direct LDMS procedure (19) is limited to conjugates with molecular mass <200 kDa. This more accurate density determination gives the *modal* number of haptens conjugated per BSA molecule (Fig. 4; Table 2) by direct observation of the mass difference. It also gives some idea of the range of hapten densities within the sample. The pairs of results for BSA are in broad agreement, and the data for all four systems show hapten densities satisfactory for immunization.

Immunization protocols using the KLH conjugates from **4** and **5** each yielded >50 mAbs which bind strongly to their respective BSA-hapten conjugates. All purified cell lines were rescreened for recognition of their hapten by using both an inhibition ELISA (24) and an SPR procedure (26). In addition to being labor intensive, the inhibition ELISA is prone to inaccuracies (27). The major error arises because the antibodies become bound to a solid phase and therefore their natural avidity contributes to their interaction with the BSA immunoconjugate bonded to the solid phase. The SPR method involves immobilizing a modified TSA (**8** or **9**), lacking the glutaryl spacer arm, to the hydrogel. Since the IgG is bound to a hydrogel which is a carboxymethylated dextran—i.e., not a true solid phase—the observed antibody affinity should not be perturbed by avidity.

This use of SPR (implemented on a Pharmacia BIAcore instrument) offers a number of benefits over the ELISA, including a reduction in assay duration and a more accurate

Table 1. Results of the TNBS screen

Conjugate	No. of haptens per protein molecule*	Hapten density, %
BSA-hapten **4**	29.1	48.5
BSA-hapten **5**	16.7	27.9
KLH-hapten **4**	330	23.1
KLH-hapten **5**	180	12.6

*Hapten numbers were calculated given that the total number of available lysines in BSA is 60 and in KLH is 1430 as estimated from the Daresbury data base (Chemical Database Service, Daresbury Laboratory, Warrington, U.K.).

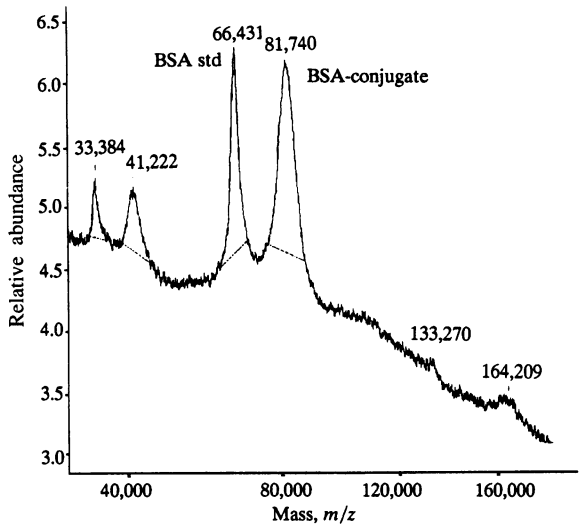

FIG. 4. An LDMS analysis of BSA-hapten **3** conjugate. A BSA internal standard is shown. The BSA conjugated was at 10 pmol/μl. The ordinate units are relative intensities.

measure of the true affinity constant K_a as opposed to the apparent affinity constant a*K*. A comparison of results from the ELISA and the SPR methods enables identification and discard of clones which recognize only the spacer arm. The results from both techniques are quite comparable: the rank orders of affinities are very similar and the majority of values of one is within 25% of the other. This outcome is somewhat surprising because it suggests either that avidity is of equal importance in both assays or that the SPR assay is sensitive to other interactions which artificially elevate the binding constant, such as "rebinding." However, when we determined dissociation kinetics of the bound antibody from the chip with increasing concentrations of TSA as opposed to pure buffer, we found that rebinding made a minimal contribution to measured K_a values.

From the large number of antibodies with a high affinity for the TSAs **4** and **5**, we have obtained several abzymes which can hydrolyze the carbamate ester bond in the nitrogen mustard prodrug **1** to generate the potent cytotoxic agent **2** (Fig. 2). These antibody catalysts have been found to reduce the viability of a human tumor cell line *in vitro* when incubated with the prodrug **1**, as shown by use of the SRB assay (25). This rapid and inexpensive *in vitro* cytotoxicity assay is highly reproducible and appears to be ideal for the rapid screening of positive clones, highlighted in preliminary binding studies, for turnover of the prodrug **1**. In essence, surviving cells are amplified by regrowth, precipitated, and stained with the anionic SRB dye. After the stained cells have been washed, the dye is released into the supernatant by raising the pH and its absorbance is measured.

A previous report has exemplified this principle by activation of a 5′-D-valyl ester prodrug of 5-fluorodeoxyuridine by an antibody that effects cytotoxicity towards a prokaryotic cell line (28). In the present work, because of its intended *in vivo* application, we used a human colorectal (LoVo) cell line in the SRB assay. The IC_{50} values of the prodrug **1** and drug **2** for the LoVo cell line were determined as 160 μM and 2 μM, respectively. This means that a concentration of 10 μM of prodrug **1** in the SRB assay would give a low background cytotoxicity (≈10%), while antibody turnover of some 20% of the prodrug **1** would generate sufficient nitrogen mustard **2** to cause ≈50% cell-kill.

Table 2. Hapten density as determined by using matrix-assisted LDMS

Conjugate	Peak *m/z*	No. of haptens per protein molecule	Hapten density, %
BSA-hapten **4**	81,740	32.1	53.5
BSA-hapten **5**	76,647	23.4	39.0

In an attempt to minimize the expense of hybridoma production of catalytic protein, both financially and in labor, we sought to demonstrate hydrolysis of the prodrug leading to cell-kill by using the hybridoma cell supernatants directly. Unfortunately, no such activity could be detected. However, when purified antibody preparations were used in the SRB assay, activity was readily identified for several mAbs elicited to either hapten, most notably for EA11-D7, DF8-D5, and BH3-B8 (see Fig. 5). Standard controls in these assays included mAb elicited to an unrelated hapten, fresh and expired media, and PBS.

A disappointingly poor correlation was found between the antibody affinity for the modified TSAs (**8** and **9**) measured by SPR and their ability to reduce cell viability in the SRB screen ($r = 0.13$). However, in light of the report by Tawfik *et al.* (29) that improved screening for catalysts can be achieved by determining the affinity of antibodies to a "short transition-state analogue," SPR displacement studies were carried out for all the clones, using the phosphonate monoester **10** as the competing ligand. The I_{50} values obtained from this study correlate much more favorably with the results of the SRB catalysis screen ($r = 0.81$; Fig. 5).

The IgG1 antibody EA11-D7, raised to hapten **4**, emerged as the most active catalyst for turnover of the carbamate prodrug **1**, and its catalytic activity has been characterized in some detail. Dose–response studies, using increasing concentrations of EA11-D7 (0.06–1.00 μM), show good linearity, while papain-derived Fab preparations of the EA11-D7 clone give catalytic activity comparable to that of the parent antibody (Fig. 6). Most significantly, the catalytic activity is fully and stoichiometrically inhibited by the TSA **6** (Fig. 6). This is consistent with the affinity of EA11-D7 for **5** of 5×10^{-9} M, determined by BIAcore assay.

The kinetics of hydrolysis of the prodrug **1** by 0.64 μM EA11-D7 were measured by following the UV absorbance change at 266 nm for a range of substrate concentrations. Initial slope measurements provided values of K_m = 201 μM and k_{cat} = 1.88 min^{-1} by nonlinear regression analysis (Fig. 7). From these data, it can be calculated that the abzyme EA11-D7 turns over ≈3 equivalents of substrate (per site) in 1 h in the SRB assay and transforms a net 4.18 μmol of prodrug **1**, which is rather more than $2 \times IC_{50}$. That analysis correlates

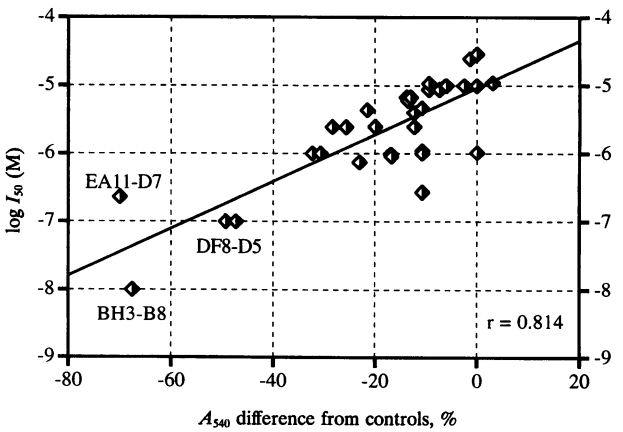

FIG. 5. A correlation of "relative" affinities (I_{50}) of the antibodies elicited to the phosphonamidate **4** to the "short transition-state analogue" **10** vs. catalytic activity (percentage absorbance change in the SRB assay relative to controls).

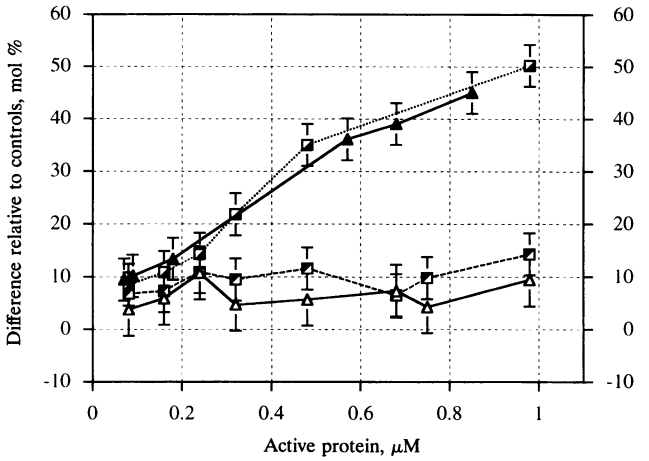

FIG. 6. Comparison between the activity of parent mAb EA11-D7 (▲) and its derived Fab (◪) in the SRB assay. The activities of both EA11-D7 and EA11-D7 Fab were studied in the presence of an equimolar concentrations of TSA **6** (△ and ◩, respectively). The concentrations of Fab and parent mAb have been adjusted for 2 catalytic sites on the parent antibody.

very well indeed with the observed net cell-kill of >70% for EA11-D7.

Since the first publications documenting antibodies as catalysts (30–32), there has been much speculation as to their potential roles in chemical synthesis and biological systems (33). One of the obstacles to their rapid development for "biological" utility has been poor catalytic power coupled with relatively high K_m values. While EA11-D7 has both k_{cat} for prodrug **1** (1.9 min^{-1}) and selectivity ratio, k_{cat}/K_m (156 $M^{-1}\cdot s^{-1}$), very much lower than those of the bacterial enzyme, CPG2, currently employed in the ADEPT system (32 s^{-1} and 6.4×10^6 $M^{-1}\cdot s^{-1}$ respectively), allowance must be made for the fact that the abzyme is working on a substrate, **2**, for which it was not designed, and this will have impaired its performance in both k_{cat} and K_m. However, in the ADEPT system, it has been suggested that a low turnover number for the catalyst could be advantageous in prolongation of the duration of drug delivery and thereby increasing the selectivity for tumor activation. Computer modeling has shown that a k_{cat} around 1.0 s^{-1} can optimize selectivity and reduce peripheral toxicity in the ADEPT system (D. Leahy, personal communication). Despite the high selectivity for concentration of the ADEPT conjugate at the tumor site, the very high ratio of total circulatory volume to tumor volume means that a significant amount of the conjugate remains in the peripheral circulation at equilibrium. Therefore, some of the prodrug is necessarily activated in the general circulation on encounter with the ADEPT conjugate. With an enzyme in the conjugate having a high turnover number, a large proportion of prodrug activation can fall under diffusion control in the periphery. By contrast, with an enzyme having a low turnover number the selectivity for activation at the tumor site is increased, leading to a reduction in peripheral toxicity. Indeed, this problem is of sufficient significance that, in some cases, antibodies to the ADEPT conjugate have been developed to effect its general destruction in plasma prior to administration of the prodrug (6). Since the turnover number for EA11-D7 approaches this target figure of 1.0 s^{-1}, it can be considered as a realistic candidate for further development in an ADAPT program in combination with carbamate-based prodrugs.

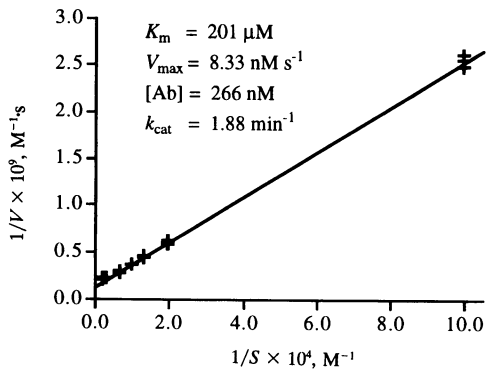

FIG. 7. Lineweaver–Burk analysis of EA11-D7-catalyzed hydrolysis of prodrug **1**. Net loss of prodrug was monitored by A_{266}.

We thank Dr. Simon Smith (Sheffield Hybridomas) for his technical assistance in hybridoma generation and the Biotechnology and Biological Sciences Research Council for provision of a Research Studentship (to P.W.) and the Engineering and Physical Sciences Research Council for a Research Studentship (to A.D.).

1. Bagshawe, K. D. (1987) *Br. J. Cancer* **56,** 531–532.
2. Bagshawe, K. D., Springer, C. J., Searle, F., Antoniw, P., Sharma, S. K., Melton, R. G. & Sherwood, R. F. (1988) *Br. J. Cancer* **58,** 700–703.
3. Bagshawe, K. D. (1990) *Biochem. Soc. Trans.* **18,** 750–752.
4. Senter, P. D., Saulnier, M. G., Schreiber, G. J., Hirschberg, D. L., Brown, J. P., Hellström, I. & Hellström, K. E. (1988) *Proc. Natl. Acad. Sci. USA* **85,** 4842–4846.
5. Senter, P. D., Schreiber, G. J., Hirschberg, D. L., Ashe, S. A., Hellstrom, K. E. & Hellstrom, I. (1989) *Cancer Res.* **49,** 5789–5792.
6. Bagshawe, K. D. (1989) *Br. J. Cancer* **60,** 275–281.
7. Lerner, R. A. & Tramontano, A. (1988) *Sci. Am.* **258** (3), 58–70.
8. Schultz, P. G. (1989) *Acc. Chem. Res.* **22,** 287–294.
9. Winter, G. & Milstein, C. (1991) *Nature (London)* **349,** 293–299.
10. Werlen, R. C., Lankinen, M., Rose, K., Blakey, D., Shuttleworth, H., Melton, R. & Offord, R. E. (1994) *Bioconjugate Chem.* **5,** 411–417.
11. Bender, M. L. & Homer, R. B. (1965) *J. Org. Chem.* **30,** 3975–3978.
12. Janda, K. D., Schloeder, D., Benkovic, S. J. & Lerner, R. A. (1988) *Science* **241,** 1188–1191.
13. Van Vranken, D. L., Panomitros, D. & Schultz, P. G. (1994) *Tetrahedron Lett.* **35,** 3873–3876.
14. Jacobsen, J. R., Prudent, J. R., Kochersperger, L., Yonkovich, S. & Schultz, P. G. (1992) *Science* **256,** 365–367.
15. Suga, H., Ersoy, O., Tsumuraya, T., Lee, J., Sinskey, A. J. & Masamune, S. (1994) *J. Am. Chem. Soc.* **116,** 487–494.
16. Altschuh, D., Dubs, M.-C., Weiss, E., Zeder-Lutz, G. & Van Regenmortal, M. H. V. (1992) *Biochemistry* **31,** 6298–6304.
17. Harlow, E. & Lane, D. P. (1988) *Antibodies: A Laboratory Manual* (Cold Spring Harbor Lab. Press, Plainview, NY), pp. 635–657.
18. Habeeb, A. F. S. A. (1966) *Anal. Biochem.* **14,** 328–336.
19. Geisow, M. J. (1992) *Trends Biotechnol.* **10,** 432–438.
20. Harlow, E. & Lane, D. P. (1988) *Antibodies: A Laboratory Manual* (Cold Spring Harbor Lab. Press, Plainview, NY), pp. 139–243.
21. Köhler, G., Howe, S. C. & Milstein, C. (1976) *Eur. J. Immunol.* **6,** 292–295.
22. Köhler, G. & Milstein, C. (1976) *Eur. J. Immunol.* **6,** 511–519.
23. Galfré, G. & Milstein, C. (1981) *Methods Enzymol.* **73,** 3–46.
24. Nieto, A., Gaya, A., Jansa, M., Moreno, C. & Vives, J. (1984) *Mol. Immunol.* **21,** 537–543.
25. Skehan, P., Storeng, R., Scudiero, D., Monks, A., McMahon, J., Vistica, D., Warren, J. T., Bokesch, H., Kennet, S. & Boyd, M. R. (1990) *J. Natl. Cancer Inst.* **82,** 1107–1112.
26. Karlsson, R., Michaelsson, A. & Mattsson, L. (1991) *J. Immunol. Methods* **145,** 229–240.
27. Goding, J. W., ed. (1986) *Monoclonal Antibodies: Principles and Practice* (Academic, London).
28. Campbell, D. A., Gong, B., Kochersperger, L. M., Yonkovich, S., Gallop, M. A. & Schultz, P. G. (1994) *J. Am. Chem. Soc.* **116,** 2165–2166.
29. Tawfik, D. S., Zemel, R. R., Arad-Yellin, R., Green, B. S. & Eshar, Z. (1990) *Biochemistry* **29,** 9916–9921.
30. Pollack, S. J., Jacobs, J. W. & Schultz, P. G. (1986) *Science* **234,** 1570–1573.
31. Tramontano, A., Janda, K. D. & Lerner, R. A. (1986) *Proc. Natl. Acad. Sci. USA* **83,** 6736–6740.
32. Tramontano, A., Janda, K. D. & Lerner, R. A. (1986) *Science* **234,** 1566–1570.
33. Lerner, R. A. (1993) *Hosp. Pract.* **28,** 53–59.
34. Leatherbarrow, R. J. (1987) ENZFIT (Elsevier, Amsterdam), Version 1.05.